Mon. Not. R. astr. Soc. (1984) **211,** 507–519

On the composition of H II regions in southern galaxies – III. NGC 2997 and 7793

M. G. Edmunds *Department of Applied Mathematics and Astronomy, University College, PO Box 78, Cardiff CF1 1XL*

B. E. J. Pagel *Royal Greenwich Observatory, Herstmonceux Castle, Hailsham, E. Sussex BN27 1RP*

Accepted 1984 June 12. Received 1984 March 12

Summary. AAT/IPCS spectra have been obtained for a part of the nuclear region and for four H II regions in the SABc galaxy NGC 2997, and for the nucleus and five H II regions in the prototype Sd Sculptor group galaxy NGC 7793. Additional observations of an H II region in the Scd galaxy NGC 300 extend previously reported results. Abundances are deduced from emission-line intensities. The abundance gradient found in NGC 7793 is very similar to that of NGC 300 and characteristic of late-type spirals, while that of NGC 2997 is milder (relative to the isophotal radius). The relationship between abundance gradients and other characteristics of spiral galaxies is discussed; the data suggest that the yield varies systematically according to local conditions, such as the surface density of stars in the disc. Calibration of line strengths in terms of abundance is discussed in an Appendix.

1 Introduction

The study of abundance gradients in galaxies, and its significance, has been reviewed by Pagel & Edmunds (1981). As part of a continuing programme of investigation of the chemical composition of H II regions in galaxies (Pagel *et al.* 1979, Paper I; Pagel, Edmunds & Smith 1980, Paper II) we present here observations of two further late-type spirals. NGC 2997, classified SABc, has a 'hotspot' nucleus (Sersic & Pastoriza 1965) and shows a bar-like structure in its inner region; it is well illustrated in the interferometric kinematic study by Milliard & Marcelin (1981). NGC 7793, in the Sculptor group (Shapley 1943), is the prototype Sd and is well illustrated by Davoust & de Vaucouleurs (1980), who have derived extensive kinematics and surface photometry (de Vaucouleurs & Davoust 1980). It is also one of the few low-mass late-type galaxies in which the CO molecule (indicative of the presence of molecular clouds) has been detected (Elmegreen, Elmegreen & Morris 1980).

H II regions in NGC 2997 are catalogued by Milliard & Marcelin (1981) and its nucleus has been studied by Osmer, Smith & Weedman (1974) and Meaburn & Terrett (1982). McCall (1982) has

Table 1. Properties of the galaxies.*

	NGC 2997	NGC 7793
α(1)	$9^h\ 43^m\ 25\overset{s}{.}5$	$23^h\ 55^m\ 14\overset{s}{.}7$
δ(1)	−30° 57′ 33″	−32° 52′ 19″
BGC(1) rev. type	SAB(rs)c	SA(s)dm
Other types	SABc	SI:SA(s)d+
D_o(1)	8.7	8.7
V_o (km s^{-1})(1)	305	214, 221(9)
Distance (Mpc)	7.6(10)‡, 10.7(8)	2.5(3), 3.1(4)‡
Linear scale of 1 arc min (kpc)	2.2	0.9
Inclination (deg)	52(1), 40(2), 38(7)	44(1), 50(5), 53(4)
Position angle of nodes (deg)	110 ± 10(2),	85(6), 95(5), 108(9)
Mass ($10^{10}M_\odot$)	4–5(2), 6–7(7)	0.3(5), 0.89(9)
R_E (disc)[11]	2.35	2.04
Group membership(3)	2997 group	Sculptor

* For NGC 300, see Paper I

\+ Preferred type: see ref (4)

‡ adopted

(1) de Vaucouleurs *et al* (1976)

(2) Milliard and Marcelin (1981)

(3) de Vaucouleurs (1975)

(4) de Vaucouleurs and Davoust (1980)

(5) Agüero (1979)

(6) Hodge (1969)

(7) Peterson (1978)

(8) from V_o with H = 75 km s^{-1} Mpc^{-1}

(9) Davoust and de Vaucouleurs (1980)

(10) Sersic (1960), from HII region diameters.

(11) McCall (1982)

made spectrophotometric observations of one H II region therein. H II regions in NGC 7793 have been catalogued by Hodge (1969), Carranza & Agüero (1977) and Davoust & de Vaucouleurs (1980), and spectrophotometric studies have been made by McCall (1982) and by Webster & Smith (1983). In addition to these two galaxies, we have supplemented our earlier work on the Scd spiral NGC 300 (Paper I) by observing an H II region closer to the nucleus than those previously reported, and we conclude this paper with a discussion of abundance gradients found in spiral galaxies in general.

General properties of the two galaxies NGC 2997 and 7793 are listed in Table 1, and details of the H II regions observed in Table 2.

2 Observations and reductions

Observations were carried out on 1978 August 28–30 (NGC 7793), 1979 November 16–18 (NGC 300, 2997 and 7793), 1981 Oct 1–5 and 1982 August 22–25 (NGC 7793) with the Anglo-Australian Telescope and UCL Image Photon Counting System and reduced using standard AAO and SPICA programs. For most observations the whole wavelength range 3400–7500 Å, was covered with a resolution of about 7 Å, but this was supplemented for some H I regions with 2 Å resolution observations of the blue spectrum 3600–4500 Å or 4200–5100 Å. In particular, this resolution was used in conjunction with combined exposures of up to 4 hr on the three outer H II regions of NGC 7793 in 1982 in order to obtain significant measurements of [O III] λ 4363. For each observation, the slit was oriented north–south and its length divided into 10 separate increments of 2.7 arcsec, allowing sky subtraction where appropriate. Slit widths were

Table 2. H II regions observed.

	Δx(1)	Δy(1)	Diameter (arc sec) (approx)	Idents	ρ(2)	ρ/ρ$_o$(3)
NGC 300(4) no 2	90	33	7	Sersic(5)52	1.77	0.18
NGC 2997(6) Nucleus(7)	0	5	3	(8)	0.12	0.03
no 3	-15	-70	3	MM 85	1.52	0.35
no 2	84	61	5	MM 306	2.07	0.48
no 1(9)	-55	113	5	MM 213/4	2.40	0.55
no 5	-32	30	5	MM 228	2.70	0.62
NGC 7793(10) Nucleus	0	0	<2		0.00	0.00
W 12(11)	-40	-9	5	DV 34? (12)	0.73	0.17
W 2	-32	-40	7	Ho 23,(13) DV 36	1.30	0.30
W 5/6	-104	-25	10	Ho 29, DV 13	1.93	0.44
W 13(9)	97	96	8	Ho 6, DV 111	3.13	0.72
DV 132	214	30	5	DV 132	3.86	0.89
W 11	248	-85	6	(14)	4.52	1.04

(1) Rectangular coordinates in arcsec relative to nucleus, increasing to E and N
(2) Distance from nucleus in arcmin, corrected for projection
(3) $\rho_o \equiv \frac{1}{2} D_o$
(4) $i = 42°$, $\Omega = 109°$ (de Vaucouleurs and Page 1962)
(5) Sersic (1967)
(6) $i = 39°$, $\Omega = 110°$ adopted
(7) Emission-line hot spot 5" North of continuum maximum (see e.g. Meaburn and Terrett 1982)
(8) Milliard and Marcelin (1981)
(9) Also observed by McCall (1982)
(10) $i = 50°$, $\Omega = 95°$ adopted
(11) Unpublished list by B L Webster
(12) Davoust and de Vaucouleurs (1980)
(13) Hodge (1969)
(14) Designated 'DV 133' by Webster and Smith (1983)

1.2 and 1.4 arcsec respectively for low and high resolution. Reddening-corrected emission-line intensities are given in Table 3; the correction assumes the reddening curve of Nandy *et al.* (1975) with a fit of case B recombination (Brocklehurst 1971) to the Balmer decrement suitably weighted in accordance with the observational errors of the lines.

3 Abundance analysis

The derivation of abundances from strong-line ratios is discussed in the Appendix; our abundances and electron temperatures deduced by these methods are given in Table 4. Where possible, electron temperatures t_r have also been deduced from the line ratios 4363/5007 ([O III]) and (with less precision) from (4068+4076)/(6717+6731) (S II]) and the agreement is satisfactory. Webster & Smith (1983) also found reasonable agreement between electron

Table 3a. Corrected line intensities in NGC 2997.

λ		f(λ)	Nucleus	No. 3	No. 2	No. 1	No. 5
3727	[O II]	0.26	.24 ± .10	.14 ± .04	.44 ± .05	.53 ± .02	.40 ± .06
3889	H8+He	0.23				-.66 .08	
3970	Hε	0.21				-.68 .08	
4102	Hδ	0.18		-.49 .08		-.60 .04	
4340	Hγ	0.135		-.33 .04	-.35 .03	-.38 .03	-.32 .08
4861	Hβ	0.00	.00 .06	.00 .02	.00 .02	.00 .02	.00 .03
4959	[O III]	-0.02			-.76 .10	-.61 .06	-.60 .10
5007	[O III]	-0.03	-.5	-.62 .08	-.27 .03	-.05 .02	-.23 .06
5876	He	-0.23				-.81 .06	
6548	[N II]	-0.34	-.37 .10	-.34 .06	-.51 .04	-.53 .05	-.44 .06
6563	Hα	-0.34	.46 .03	.46 .02	.45 .01	.45 .02	.46 .03
6584	[N II]	-0.34	.02 .06	.03 .04	.00 .02	-.16 .02	-.06 .04
6717	[S II]	-0.36	-.26 .08	-.43 .06	-.45 .04	-.66 .08	-.27 .06
6731	[S II]	-0.36	-.29 .08	-.45 .06	-.59 .04	-.92 .10	-.38 .06
C			1.24	.70	1.43	.68	.84
log I (Hβ)*			-13.9	-14.3	-13.6	-14.0	-14.2
EW (Hβ), Å			10	90	70	100	>50

*Rough value of specific intensity, in ergs cm^{-2} arcsec^{-2}, in strongest increment, corrected for absorption.

Table 3b. Corrected emission-line intensities in NGC 300 and 7793.

λ		f(λ)	NGC 300 no 2	Nucleus	W 12	W 2	NGC 7793 W 5/6	W 13	DV 132	W 11
3727	[O II]	0.26	.47 ± .10	.30 ± .03	.32 ± .04	.48 ± .03	.52 ± .02	.65 ± .08	.32 ± .05	.50 ± .05
3771	H 11	0.26								-1.28 .08
3798	H 10	0.25	-1.40 .10							-1.32 .06
3835	H 9	0.24	-1.17 .06		-.80 .20			-1.09 .08		-1.14 .06
3869	[Ne III]	0.24	-1.60 .10					-.90 .20	-.48 .10	-.90 .04
3889	H8+He	0.23	-.80 .04		-.60 .20			-.71 .04		-.71 .04
3970	Hε	0.21	-.91 .03			-.80 .15		-.76 .15		-.82 .04
4068/76	[S II]	0.19	-1.6 .1					-1.50 .20		-1.66 .22
4102	Hδ	0.18	-.66 .04		-.60 .03	-.65 .09	-.60 .15	-.61 .04	-.66 .12	-.61 .03
4340	Hγ	0.135	-.37 .02	-.33 .04‡	-.35 .02	-.37 .05	-.40 .10	-.31 .02	-.32 .07	-.34 .0
4363	[O III]	0.13	<-2.07					-1.7 ± .2	-1.75 ± .10	-1.98 .06
4471	He	0.10	-1.55 .08					-1.58 ± .07	-1.46 ± .05	-1.48 .02
4861	Hβ	0.00	.00 .02	.00 .02‡	.00 .02	.00 .03	.00 .04	.00 .02	.00 .07	.00 .0
4959	[O III]	-0.02	-.61 .06	-.81 .05		-.25 .04	-.63 .09	-.27 .02	.00 .07	-.10 .02
5007	[O III]	-0.03	-.20 .03	-.40 .04	-.74 .11	.20 .03	-.22 .04	.23 .01	.48 .06	.40 .03
5876	He	-0.23			-1.04 .20			-1.01 .20		-1.08 .18
6548	[N II]	-0.34	-.87 .08	-.58 .04	-.79 .15			-.89 .09		-1.04 .18
6584	[N II]	-0.34	-.25 .04	-.10 .04	-.18 .04	-.50 .07	-.37 .07	-.35 .04	-.44 .23	-.69 .07
6563	Hα	-0.34	.41 .04	-.47 .02	.47 .02	.47 .03	.46 .02	.47 .01	.42 .06	.45 .01
6717	[S II]	-0.36	-.33 .05	-.57 .04	-.65 .12	-.72 .10	-.40 .06	-.43 .09	<-.44	-.83 .09
6731	[S II]	-0.36	-.55 .05	-.64 .04	-.88 .20	-1.00 .15	-.51 .08	-.58 .05	<-.31	-1.00 .13
C			.40	1.00	.60	1.25	1.00	.60	.55	.45
log I (Hβ)*			-14.6	-13.9	-14.4	-13.6	-14.1	-14.5	-14.6	-14.7
EW (Hβ), Å			70	1.4	100:			80	100	60

*Rough value of specific intensity in strongest increment, in ergs cm^{-2} arc sec^{-2}, corrected for absorption
‡Absorption in underlying continuum, resolved at high dispersion

temperatures from λ 4363 (where it could be measured) and from strong-line ratios. Implications of the abundances for galactic chemical evolution are explored in Section 5.

4 Nuclear spectra

As can be seen from the direct photographs by Osmer, Smith & Weedman (1974), Calderón & Sérsic (1979) and Meaburn & Terrett (1982), and the latter's IPCS spectra, the nuclear region of NGC 2997 consists of an amorphous nucleus proper, consisting of a red stellar population without emission lines, surrounded by six or so emission-line knots arranged in a tightly wound spiral or ring with a radius of about 4 arcsec≡200 pc in the plane of the system. Spectrophotometry by Meaburn & Terrett shows that the south-eastern hotspot, designated by them as X, is a low-excitation H II region with a hot-star continuum and almost no reddening (C=0.15); the south-western hotspot Z could be similar but their spectrum is very noisy in this case.

Table 4a. Abundances in NGC 300 and NGC 2997.

	NGC 300	NGC 2997				
	no 2	Nucleus	no 3	no 2	no 1	no 5
12+log (O/H) from [O III]/Hβ	8.80	> 9.0	9.09	8.86	8.72	8.82
" " [O III]/[N II]	8.95	> 9.0	9.10	8.90	8.72	8.90
" " ([O II] + [O III])/Hβ	8.73	9.14 ± .05	9.20	8.79	8.62	8.80
12+log (O/H) adopted	8.80 ± .10	9.15 ± .20	9.20 ± .20	8.79 ± .20	8.62 ± .20	8.80 ± .20
<t> from emissivity	0.72 ± .05‡	0.59 ± .05	0.56 ± .05	0.72 ± .05	0.81 ± .05	.70 ± .05
$O^{2+}/(O^{+} + O^{2+})$	.04	<0.07	0.07	.10	.15	.12
log O/N	1.35 ± .12	1.01 ± .12	0.96 ± .10	1.03 ± .10	1.13 ± .10	.96 ± .10
log H/He	1.26 ± .10				.97 ± .07	
log O^{2+}/Ne^{2+}	0.82 ± .12					
log O/Ne	0.8					

‡t_r ([O III]) <1.29; t_r ([S II]) = .70 ± .08; <t> (adopted) = 0.71 ± .04

Table 4b. Abundances in NGC 7793.

	Nucleus	W12	W2	W5/6	W13	DV 132	W11
12+log(O/H) from t_r(O III)					8.02±.3	8.32	8.54
12+log(O/H) from [O III]/Hβ	8.94	9.18	8.56	8.83	8.53	8.37	8.43
" " [O III]/[N II]	8.92	9.06	8.53	8.72	8.57	8.46	8.44
" " ([O II]+[O III])/Hβ	8.98	9.03	8.56	8.67	8.38	8.47	8.42
12+log (O/H) adopted*	8.98	9.03	8.56	8.67	8.38	8.40	8.48
<t> from emissivity	.63±.05	.62±.05	.83±.10	.78±.09	.98±.12	.88±.10	.93±.11
t_r ([O III])					1.22±.20	0.95±.07	.87±.05
t_r ([S II])					.83±.20		1.25±.30
<t> adopted	.63±.05	.62±.05	.83±.10	.78±.09	.94±.10	.92±.07	0.90±.05
$O^{2+}/(O^{+}+O^{2+})$	.10	.04	.28	.11	.25	.51	.37
log O/N	1.14±.11	1.25±.12	1.43±.14	1.40±.14	1.35±.13	1.16±.30	1.55±.12
log H/He		1.22±.20			1.15±.20		1.17±.08
log O^{++}/Ne^{++}					0.66	0.44	0.79
log O/Ne					0.6	0.4	0.7

*Estimated error ± 0.20

Spectrophotometry of the entire $(20\,\text{arsec})^2$ nuclear region by Osmer *et al.* also indicates a low-excitation H II region, but their $H\alpha/H\beta$ ratio implies a very severe reddening ($C=1.7$). Our IPCS spectra cover the nucleus and the emission-line hotspot 3 arcsec to the north; apart from more severe reddening ($C=1.2$, approaching OSW), our relative line intensities in this hotspot are in good agreement with those found by Meaburn & Terrett in their region X. We conjecture that all the hotspots in the ring are conventional low-excitation H II regions ionized by hot stars and that the nucleus itself is not currently 'active'; the chemical composition of the H II region is quite normal, while the nucleus itself shows Mg I and other absorption features typical of an old, metal-rich stellar population (*cf.* Meaburn & Terrett 1982).

The nucleus of NGC 7793 is typical of the nuclei of late-type galaxies, both in its appearance on direct photographs (de Vaucouleurs & Davoust 1980) and in its spectrum, which resembles those of other late-type spiral nuclei such as NGC 4559 (Alloin 1973) or NGC 5248 (McClure, Cowley & Crampton 1980). The continuous and absorption-line spectrum, and the nature of the underlying stellar population, have been discussed elsewhere (Dîaz *et al.* 1982). The emission line spectrum appears to be that of an ordinary H II region with solar abundances (*cf.* Table 4b).

5 Abundances in H II regions and the chemical evolution of galaxies

Most theories of abundance gradients in spirals depend on the basic gas-fraction effect discussed by Searle & Sargent (1972). In the simple one-zone model, as long as instantaneous recycling is a good approximation, the heavy-element abundance is given by the relation

$$Z=p\ln(m/g) \qquad (1)$$

where the 'yield' p is a quantity characteristic of the initial mass function, m is the mass of the zone and g the mass of residual gas, assuming that p is constant and that the system consisted initially of pure gas with no heavy elements. As long as the surface density of gas increases inwards towards the centres of galaxies more slowly than the total surface density, an abundance gradient is to be expected in a disc-like galaxy that can be considered to be stratified in isolated concentric cylindrical zones (*cf.* Pagel 1981).

The introduction of dynamical collapse (Lynden-Bell 1975; Larson 1976; Tinsley & Larson 1978; Chiosi 1980) or metal-enhanced star formation (Talbot & Arnet 1975) enables one to explain the metallicity distribution of stars near the Sun, but plausible models so far suggested

seem to cause only minor modifications of the basic abundance gradient in the interstellar gas predicted from gas-fraction arguments using equation (1). More significant modifications arise when there are radial flows of gas, e.g. due to infall of gas with low angular momentum (Mayor & Vigroux 1981). A simple two-zone model which mimics dynamical collapse or radial inflow (Edmunds & Morgan, in preparation) suggests that, if equation (1) is applied, the effective value of the yield will become variable.

The gas-fraction effect was investigated by Pagel *et al.* (1978) for the Magellanic Clouds and outer regions of our Galaxy, M33 and M101, and by Lequeux *et al.* (1979) and Kinman & Davidson (1981) for irregular and compact galaxies, with fairly encouraging results; in addition both Lequeux *et al.* and Kinman & Davidson found that abundances (and inverse gas fractions) in irregular galaxies increase systematically with the total mass. In the meantime, additional data on spiral galaxies have become available from: the work reviewed in Pagel & Edmunds (1981), the studies of H II regions in M31 by Dennefeld & Kunth (1981) and Blair, Kirshner, & Chevalier (1982), additional observations of M33 (Kwitter & Aller 1981), M101 (Sedwick & Aller 1981; Rayo, Peimbert & Torres-Peimbert 1982) and NGC 1365 (Alloin *et al.* 1981); the present work; and especially the extensive observations of McCall (1982), who also provides a most valuable compilation of galactic structural data including stellar and H I surface densities, so that a fresh discussion is opportune.

Abundance gradients are often presented in the form of a plot of log (O/H) against ϱ/ϱ_0 where ϱ is the radial distance from the centre and ϱ_0 an isophotal radius (either de Vaucouleurs or Holmberg). Such a plot for various galaxies (e.g. Pagel & Edmunds 1981) gives a narrow range of abundances in the nuclei, but a much wider range at the outer isophote, where the oxygen abundance is correlated with the morphological type (and mean surface brightness and colour) of the underlying galaxy. If, as recommended by McCall, ϱ_0 is replaced by the effective radius ϱ_E of the exponential disc, then a much more uniform picture is obtained (Fig. 1). There is no perceptible intrinsic scatter among Scd and Sd galaxies and earlier-type galaxies show some scatter, but (with the possible exception of NGC 4736 and 1365) have on average a similar gradient and an oxygen abundance only a factor of 2 higher at each normalized radius. [Following McCall and Appendix 1, our largest abundances are now a factor of 2 lower than those given with colons in Pagel & Edmunds (1981) but for $12+\log(O/H)<9.2$ we continue to use the calibration by Pagel, Edmunds & Smith (1980).]

A similar picture emerges when we plot abundances against surface mass density σ_d of stars in the disc (Fig. 2). The surface mass densities have been derived by McCall following a method due to Monnet & Simien (1977) which assumes that the mass distributions in the bulge and disc follow the corresponding light distributions; with this assumption the rotation curve is fitted with just two parameters, namely the mass-to-light ratios of the bulge and the disc respectively. Thus the effect of unseen halo material (which may or may not affect chemical evolution) is not explicitly taken into account except through its indirect influence on derived mass-to-light ratios. This probably does not impair the physical significance of σ_d because in typical observed spirals there is a nearly unique relation between the surface brightness and the total mass surface density (Petrou 1981). Inspection of Fig. 2 shows that there is a well-defined average line for Scd galaxies and that this same line essentially forms a lower envelope to the abundances found in galaxies of earlier morphological type. This difference between Scd and earlier-type galaxies has already been noted by McCall (1982).

The galactic structural quantity offering the most straightforward interpretation when compared with abundances is the gas fraction (see Fig. 3), data for calculating which have again been assembled by McCall. Unfortunately such data are subject to some uncertainty (1) because only atomic hydrogen has been quantitatively measured giving a surface density $\sigma_{H\,I}$ and an unknown amount must be added to $\sigma_{H\,I}$ to allow for H_2 molecules; and (2) because in the outer

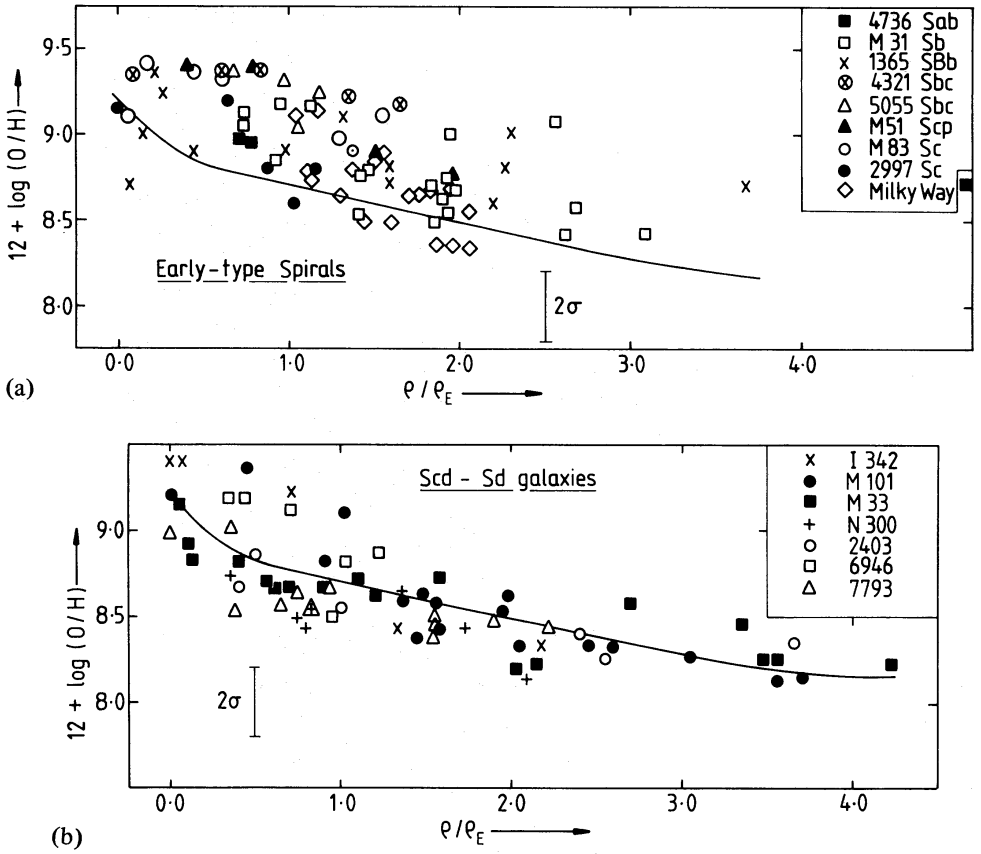

Figure 1. Plot of oxygen abundance against galactocentric distance, normalized by the effective radius ϱ_E of the disc taken from McCall (1982). (a): Early-type spirals from McCall (1982), references quoted in text and this paper. Abundances in the Milky Way Galaxy are from Shaver *et al.* (1983). The Sun is shown by the usual symbol. (b): Late-type spirals from the same sources.

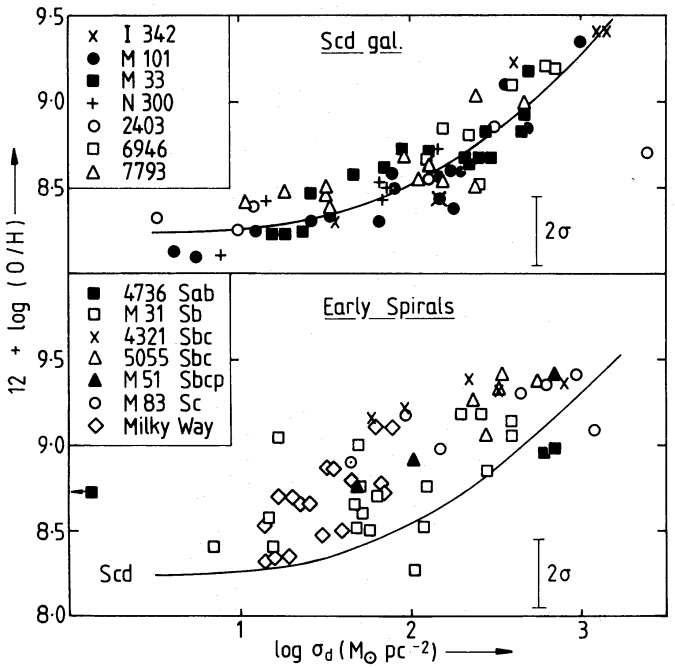

Figure 2. Plot of oxygen abundance against surface mass density of stars σ_d taken from McCall (1982). The eye-fit curve to the Scd data points in Fig. 2b is repeated for comparison purposes in Fig. 2a.

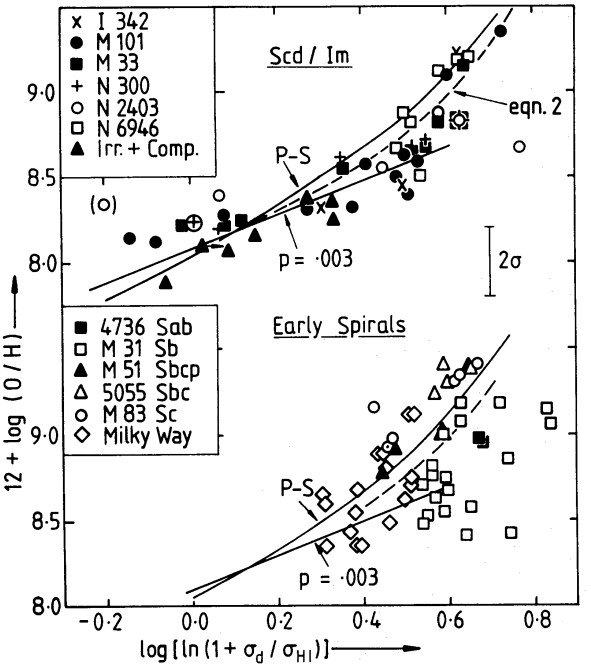

Figure 3. Log plot of oxygen abundance against the logarithm of the H I gas fraction for spiral galaxies; filled triangles in the upper panel represent irregular and compact galaxies after Lequeux *et al.* (1979), with the ratio of total mass to H I mass as abscissa. Straight lines represent the simple model with a yield of 0.003, assuming $Z=25$ (O/H), while the curved solid lines represent the variable-yield model of Peimbert & Serrano (1982) and the curved broken lines equation (2).

parts of spiral discs the total surface density is low and uncertain, being obtained from an extrapolation of the exponential law for stars, with H I added. It is possible for the disc surface density to have been underestimated in this regime and the corresponding points plotted too far to the left. Conversely, whenever molecular hydrogen is important, the points are plotted too far to the right. Bearing in mind the uncertainties, there seems to be a relationship between abundances and gas fraction for the Scd and irregular galaxies: a constant yield near 0.003 fits many of the data, but a better fit is provided by the hypothesis of Peimbert & Serrano (1982) that the yield increases with metallicity.* In the case of early-type spirals, we believe that the points plotted for the extreme inner and outer parts of M31, where the H I surface density is abnormally low, may be affected by H_2 molecules and ionization by the intergalactic radiation field, respectively. The other H II regions shown in both panels of Fig. 3 are in environments with more typical H I column densities of about $7\,M_\odot\,\mathrm{pc}^{-2}$, although the CO data reviewed by Solomon (1983) suggest that M51 and NGC 6946 should be affected the most, and M31 should be affected the least, by the correction for molecules! The conversion from ^{12}CO brightness to H_2 column density is still not well established, however (Li, Riley & Wolfendale 1983). Discounting M31, then, the variable-yield model of Peimbert & Serrano seems to give a good fit to the data now available for irregular and spiral galaxies of all types. However, this does not mean that we should necessarily accept Peimbert & Serrano's mechanism whereby the yield increases because it is affected by the metallicity directly and therefore increases with time in any given region; this could perhaps happen, but would exacerbate the 'G-dwarf' problem arising from the narrow

*There are calibration uncertainties here. McCall finds a good fit to $p=0.01$ for Scd spirals, but this results from his calibration at intermediate abundances and he ignores irregular galaxies. Rayo *et al.* (1982) suggest, by contrast, that the highest abundances result from overestimates by us (and hence by McCall) and, if they were right, then $p\simeq0.003$ would fit all the data for Scd and irregular Galaxies. However, the data of Rayo *et al.* so far as they go, merely confirm our calibration from Papers I and II (*cf.* Appendix).

distribution of metallicities in stars of the solar neighbourhood (e.g. Pagel 1981). It is at least equally plausible that the yield is constant with time in any one region, but depends on local conditions such as the total surface density. If, for example, we assume

$$p=0.003+7\times10^{-6}\sigma_{\rm d} \qquad (2)$$

($\sigma_{\rm d}$ in $M_\odot\,{\rm pc}^{-2}$), then we obtain (except in the case of M31) points lying close to the broken curves in Fig. 3, which fit the data about equally well. We are thus tempted to conclude that the data favour a one-zone model with a spatially or temporally variable yield that is fixed by local conditions, though whether it is the metallicity that drives the yield or vice versa is unclear. [Under 'one-zone model' we mean to include dynamical collapse models which lead to a similar relationship between gas-phase abundance and gas fraction.] The existence of an inward-increasing yield in our own galaxy has also been suggested by Güsten & Mezger (1982).

How unique is this conclusion? If a constant yield is assumed, then a one-zone model is not viable (unless our calibration of strong spectral features is wildly wrong), but radial inflow of the sort considered by Mayor & Vigroux (1981) can enhance the abundance gradients to the observed level by enriching inner zones of the disc at the expense of the outer zones. When all galaxies are taken together, however, this is not a very good description of what we observe, since we find that a large surface density and/or inverse gas fraction leads to a high abundance whether it be found in the outer parts (as in 6946, M51, M83) or the inner parts of the optical galaxy, and vice versa (e.g. 7793 nucleus). Furthermore, even an inflow model, with a constant yield, cannot reconcile the abundances found in the outer parts of M51 and M83, on the one hand, with those found in irregular galaxies on the other. The yield, then, has to vary from one place to another and its value seems to be a well-defined function of local conditions such as the total surface density and gas fraction – particularly in the case of Scd galaxies, where the disc is most dominant. It follows, then, either that inflow does not have a marked influence on abundance gradients in spiral galaxies, or that inflow is part of a determinate pattern that fixes the run of all parameters including surface density, gas fraction, yields and abundances.

Acknowledgments

We thank the SERC Panel for Allocation of Telescope Time for assigning time on the AAT for this investigation; the Director and staff of the AAO for their cooperation; Roberto Terlevich for his helpful suggestions; Marshall L. McCall, Manuel Peimbert and colleagues and Louise Turtle and Malcolm Smith for communicating their results in advance of publication; and Angeles Díaz for assistance with data reduction.

References

Agüero, L., 1979. *Astrophys. Space Sci.*, **65,** 423.
Alloin, D. 1973. *Astr. Astrophys.*, **27,** 433.
Alloin, D., Collin-Souffrin, S., Joly, M. & Vigroux, L., 1979. *Astr. Astrophys.*, **78,** 200.
Alloin, D., Edmunds, M. G., Lindblad, P. O. & Pagel, B. E. J., 1981. *Astr. Astrophys.*, **101,** 377.
Blair, W. P., Kirshner, R. P. & Chevalier, R., 1982. *Astrophys. J.*, **254,** 50.
Borsenberger, J. & Stasinska, G., 1981. *Astr. Astrophys.*, **106,** 158.
Brocklehurst, M., 1971. *Mon. Not. R. astr. Soc.*, **153,** 471.
Calderón, J. H. & Sérsic, J. L., 1979. *Observatory*, **99,** 215.
Carranza, G. & Agüero, E., 1977. *Astrophys. Space Sci.*, **43,** 397.
Chiosi, C., 1980. *Astr. Astrophys.*, **83,** 206.
Davoust, E. & de Vaucouleurs, G. 1980. *Astrophys. J.*, **242,** 30.
Dennefeld, M. & Kunth, D. 1981. *Astr. J.*, **86,** 989.
Díaz, A. I., Edmunds, M. G., Pagel, B. E. J. & Phillips, M. M., 1982. *Mon. Not. R. astr. Soc.*, **201,** 49P.
Dufour, R. J., Talbot, R. J., Jensen, E. B. & Shields, G., 1980. *Astrophys. J.*, **236,** 119.

Elmegreen, B. G., Elmegreen, D. M. & Morris, M., 1980. *Astrophys. J.,* **240,** 455.
French, H. B., 1980. *Astrophys. J.,* **240,** 41.
French, H. B. & Miller, J., 1981. *Astrophys. J.,* **248,** 468.
Güsten, R. & Mezger, P. G., 1982. *Vistas in Astr.,* **26,** 159.
Hodge, P. W. 1969. *Astrophys. J. Suppl.,* **18,** 73.
Jensen, E. B., Strom, K. M. & Strom, S. E., 1976. *Astrophys. J.,* **209,** 748.
Kinman, T. D. & Davidson, K., 1981. *Astrophys. J.,* **243,** 127.
Kunth, D. & Sargent, W. L. W., 1983. *Astrophys. J.,* **273,** 81.
Kwitter, K. B. & Aller, L. H., 1981. *Mon. Not. R. astr. Soc.,* **195,** 939.
Larson, R. B., 1976. *Mon. Not. R. astr. Soc.,* **176,** 31.
Lequeux, J., Peimbert, M., Rayo, J. F., Serrano, A. & Torres-Peimbert, S., 1979. *Astr. Astrophys.,* **80,** 155.
Li, T. P., Riley, P. A. & Wolfendale, A., 1983. *Mon. Not. R. astr. Soc.,* **203,** 87.
Lynden-Bell D., 1975. *Vistas in Astr.,* **19,** 299.
Mayor, M. & Vigroux, L., 1981. *Astr. Astrophys.,* **98,** 1.
McCall, M. L., 1982. *Thesis,* University of Texas, Austin.
McClure, R. D., Cowley, A. P. & Crampton, D., 1980. *Astrophys. J.,* **236,** 112.
Meaburn, J. & Terrett, D. L., 1982. *Mon. Not. R. astr. Soc.,* **200,** 1.
Milliard, B. & Marcelin, M., 1981. *Astr. Astrophys.,* **95,** 59.
Monnet, G. & Simien, F., 1977. *Astr. Astrophys.,* **56,** 173.
Nandy, K., Thompson, G. E., Jamar, C., Monfils, A. & Wilson, R., 1975. *Astr. Astrophys.,* **44,** 195.
Osmer, P. S., Smith, M. G. & Weedman, D. W., 1974. *Astrophys. J.,* **192,** 279.
Pagel, B. E. J., 1981. *The Structure and Evolution of Normal Galaxies,* p. 211, eds Fall, D. M. & Lynden-Bell, D. Cambridge University Press.
Pagel, B. E. J. & Edmunds, M. G., 1981. *Ann. Rev. Astr. Astrophys.,* **19,** 77.
Pagel, B. E. J., Edmunds, M. G., Blackwell, D. E., Chun, M. S. & Smith, G., 1979. *Mon. Not. R. astr. Soc.,* **189,** 95 (Paper I).
Pagel, B. E. J., Edmunds, M. G., Fosbury, R. A. E. & Webster, B. L., 1978. *Mon. Not. R. astr. Soc.,* **184,** 569.
Pagel, B. E. J., Edmunds, M. G. & Smith, G., 1980. *Mon. Not. R. astr. Soc.,* **193,** 219 (Paper II).
Peimbert, M. & Serrano, A., 1982. *Mon. Not. R. astr. Soc.,* **198,** 563.
Peterson, C. J., 1978. *Astrophys. J.,* **226,** 75.
Petrou, M., 1981. *Mon. Not. R. astr. Soc.,* **196,** 933.
Rayo, J. F., Peimbert, M. & Torres-Peimbert, S., 1982. *Astrophys. J.,* **255,** 1.
Searle, L. 1971. *Astrophys. J.,* **168,** 327.
Searle, L & Sargent, W. L. W., 1972. *Astrophys. J.,* **173,** 25.
Sedwick, K. E. & Aller, L. H., 1981. *Proc. Nat. Acad. Sci.,* **78,** 1994.
Sérsic, J. L., 1960. *Z. Astrophys.,* **50,** 168.
Sérsic, J. L., 1967. *Z. Astrophys.,* **64,** 212.
Sérsic, J. L. & Pastoriza, M. G., 1965. *Publ. Astr. Soc. Pacific,* **77,** 287.
Shapley, H., 1943. *Galaxies,* p. 29, Blakiston, Philadelphia.
Shaver, P. A., McGee, R. X., Danks, A. C. & Pottasch, S. R., 1983. *Mon. Not. R. astr. Soc.,* **204,** 53.
Shields, G. & Searle, L., 1978. *Astrophys. J.,* **222,** 821.
Solomon, P. M., 1983. *Internal Kinematics and Dynamics of Galaxies, IAU Symposium no. 100,* ed. Athanassoula, E.
Stasinska, G. 1980. *Astr. Astrophys.,* **84,** 320.
Stasinska, G., Alloin, D., Collin-Souffrin, S. & Joly, M., 1981. *Astr. Astrophys.,* **93,** 36.
Talbot, R. J. & Arnett, W. D., 1975. *Astrophys. J.,* **197,** 551.
Tinsley, B. M. & Larson, R. B., 1978. *Astrophys. J.,* **221,** 554.
de Vaucouleurs, G. 1975. *Stars and Stellar Systems, 9: Galaxies and the Universe,* p. 557, eds Sandage, A. R., Sandage, M. & Kristian, J., University of Chicago Press.
de Vaucouleurs, G. & Davoust, E. 1980. *Astrophys. J.,* **239,** 783.
de Vaucouleurs, G. & Page, J., 1962. *Astrophys. J.,* **136,** 107.
de Vaucouleurs, G., de Vaucouleurs, A. & Corwin, H. G., 1976. 2nd Reference Catalogue of Bright Galaxies, Monographs in Astronomy no. 2, Texas, U.T. Press.
Webster, B. L. & Smith, M. G. 1983. *Mon. Not. R. astr. Soc.,* **204,** 743.

Appendix: Abundances in H I regions and strong-line ratios

Inspired by the original suggestion of Searle (1971) that large-scale radial gradients in the line ratios [O III]/Hβ and Hα/[N II] in giant H II regions of late-type spirals are primarily due to

abundance gradients, several authors have used such ratios of strong lines to guess abundances in H II regions where temperature-sensitive lines like [O III] λ 4363 are too weak to be detected. This is sometimes known as the empirical method, first used in the form of an uncalibrated ranking by Jensen, Strom & Strom (1976), on the basis of [O III] λ 5007/Hβ. The work of Shields & Searle (1978) provided a calibration point for such empirical methods at the high-abundance end where λ 4363 can never be measured, whereas numerous measurements of 4363 and other weak temperature-sensitive lines are available for low-abundance H II regions in irregular galaxies and the outer parts of Scd spirals. Accordingly, Alloin *et al.* (1979) put forward a calibration of the electron temperature against the readily observable line ratio [O III]/[N II] whereas Pagel *et al.* (1978, Paper I) suggested, on various grounds, using ([O II]+[O III])/Hβ, for which they gave calibrations of both oxygen abundance and electron temperature. Following model calculations by Dufour *et al.* (1980), Pagel, Edmunds & Smith (1980, Paper II) extended their calibration to higher oxygen abundances and gave curves relating the oxygen abundance to all three line ratios [O III]/Hβ, [O III]/[N II] and ([O II]+[O III])/Hβ, estimating a typical precision of $\pm$0.2 dex in log O/H and about $\pm$0.1 dex in log N/O (assuming a mean electron temperature such as to give the adopted O-abundance from [O II] and [O III] and that $N/O=N^+/O^+$). The precision attainable by these methods has also been discussed by Stasinska *et al.* (1981). Their validity depends on the existence of at least a statistical relationship between the effective temperatures of the hottest stars in the ionizing cluster and the oxygen abundance and while such a relationship undoubtedly

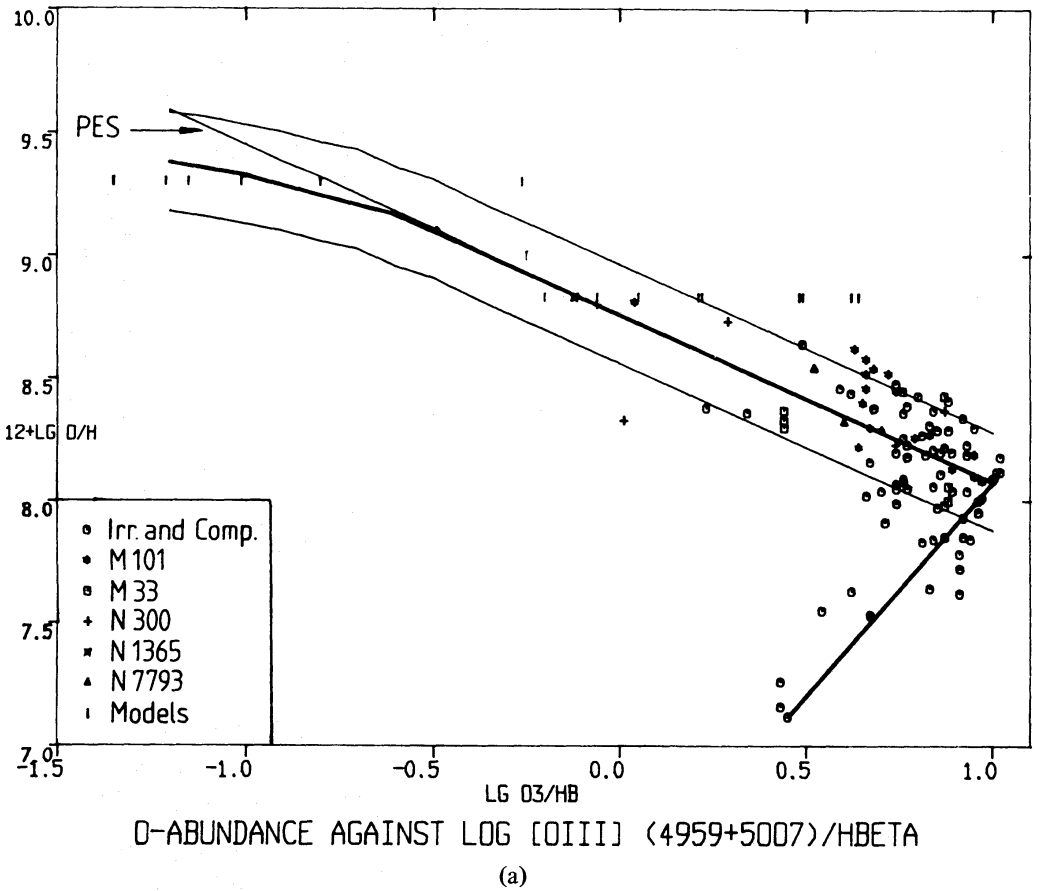

(a)

Figure A1. 12+log (O/H) against (a) log [O III] (4959+5007)/Hβ; (b) log [O III] 5007/[N II] 6584; (c) ([O II] 3727+[O III] 4959+5007)/Hβ. The lines flanked by parallel lines $\pm$0.2 dex above and below represent the adopted calibrations, which are identical with PES for 12+log O/H$\leq$9.1 but assume somewhat lower abundances above and to the left of this point.

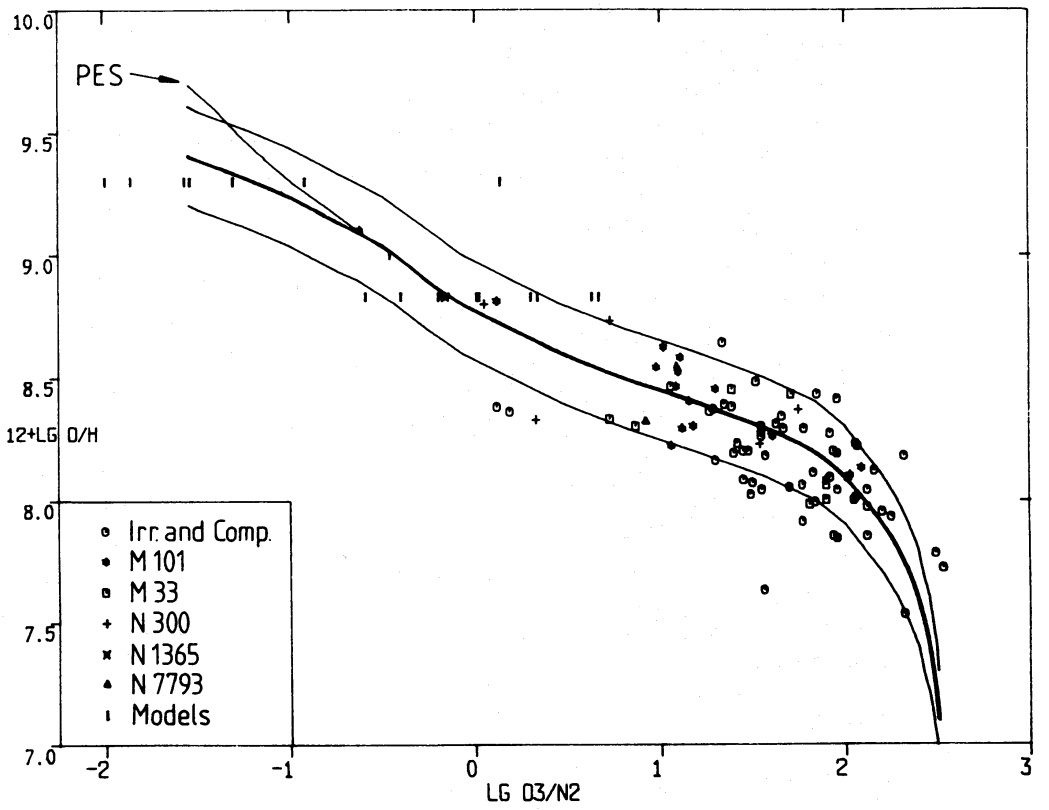

OXYGEN ABUNDANCE AGAINST LOG [OIII]/[NII]

(b)

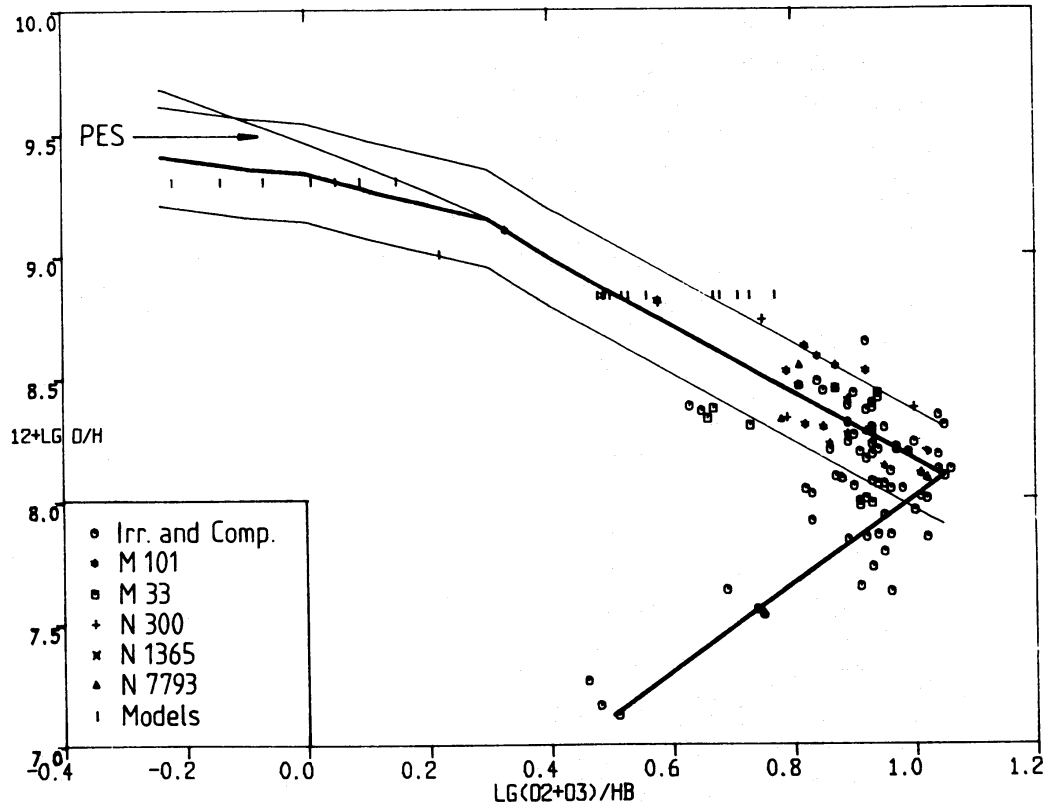

OXYGEN ABUNDANCE AGAINST LOG(OII+OIII)/HBETA

(c)

applies to many objects, its universality has not been established; furthermore, inhomogeneous structure may introduce large errors in some cases.

Since the appearance of Paper II, there have been further model computations by Stasinska (1980), Borsenberger & Stasinska (1981) and McCall (1982) and further observations of calibrating objects (French 1980; French & Miller 1981; Kinman & Davidson 1981; Kwitter & Aller 1981; Sedwick & Aller 1981; Rayo *et al.* 1982; Kunth & Sargent 1983; Shaver *et al.* 1983; Webster & Smith 1983; and this paper), making a re-appraisal of the calibration worth while. The new observational data (Fig. A1) confirm the PES curves for $12+\log O/H \leqslant 9.1$, but at lower excitation the new models of both Stasinska and McCall suggest slightly lower oxygen abundances than had been adopted by PES on the basis of the models by Dufour *et al.* (1980). We accordingly adopt the slightly flatter curves of Fig. A1, bearing in mind, however, that the uncertainties in the calibration are great at this end even if the ranking of H II regions according to abundance is good.